

International Journal of Emerging Multidisciplinaries: Mathematics

Research Paper

Journal Homepage: www.ijemd.com

ISSN: 2790-1998 (print), 2790-3257 (online)

Effects of Thermal Radiation on Jeffery Hamel Flow For Stretchable Walls of Newtonian Fluid: Analytical Investigation

¹Adnan Abbasi, Umar Khan^{2,*}, Naveed Ahmed³, Basharat Ullah¹

¹Department of Mathematics, Mohi-ud-Din Islamic University, Nerian Sharif AJ&K, Pakistan

²Department of Mathematics and Statistics, Hazara University, Mansehra, Pakistan

³Department of Mathematics, HITEC University Taxila Cantt, Pakistan

*Corresponding author

Abstract

A viscous, incompressible fluid flows between two inclined planar walls. The walls are able to extend and decrease in size. By substituting an appropriate dimensionless variable, the dimensional partial differential equations of the flow model can be transformed into nondimensional ordinary differential equations. Solving nondimensional velocity and temperature in the model is made possible by the use of an analytical approach known as Adomian's decomposition (AD). Runge-Kutta techniques of order four are used to calculate numerical solutions to ensure the correctness of the analytical answer. On velocity and temperature, the impact of several dimensionless physical quantities embedded in the flow model is visualized graphically. The possibility of contracting or expanding a wall is considered. Finally, some final thoughts on this work.

Keywords: Jeffery-Hamel flow, Stretching/Shrinking walls, Runge-Kutta scheme, Adomian's decomposition method, nonlinear ordinary differential equations.

1. Introduction

To investigate the flow between convergent and divergent channels, Jeffery [1] and Hamel [2] were the first to do so. Jeffery-Hamel flow is the name given to the phenomenon after them. Two non-parallel walls are separated by an angle of 2α by a flow of viscous, incompressible fluid. The flow between the walls is caused by a source at the junction of the walls. Because of the wide variety of businesses that might benefit

from this flow, its importance cannot be overstated. Mechanical, civil, environmental, chemical, and aeronautical engineering are just a few examples.

Research in magnetohydrodynamics, thermal radiations, and heat transfer is a major focus because of the numerous industrial and practical applications. An investigation of heat transfer and magnetohydrodynamic effects on nanofluids in converging/diverging channels by Mohyud-Din et al. [3] was published in 2015. With regard to converging/diverging channels, Khan et al. examined the influence of slip-on water-based nanofluid flow. To better understand the impact of thermal radiation on second-grade fluid flow, Hamed Ziaei Poor [5] conducted a study in 2014. They looked at the electrically conducting fluid between the convergent/divergent channels. They used the Differential Transform Method (DTM) to solve the flow model analytically and discovered excellent agreement between the analytical and numerical solutions. A second-grade fluid flow was studied by Hayat et al. [6] in the presence of convergent/divergent channels. Homotopy Analysis was used to solve the problem. [6].

It was only recently that U. Khan et al. [7] investigated the issue of viscous, incompressible fluid in convergent/divergent channels. Adomian's decomposition method and the effects of Soret, Dufour, and chemical reactions were examined for the solution of the flow model. Achieving accurate solutions in non-linear flow models is a remarkable achievement. Many authors use series solutions to solve their problems. Many analytical techniques were used to accomplish this, including the Variational Iteration Method (VIM) [8, 9], the Variation of Parameters (VPM) [12, 13], the Adomian's decomposition method (ADM) [15, 16, 17], the Homotopy Analysis Method (HAM) [19, 20, 21], the Differential Transform Method (DTM) [23, 24, 25], and the Homotopy perturbation method (HPM) [26, 27].

Research into magnetohydrodynamics and thermal radiation effects on viscous incompressible fluid flow between nonparallel inclined plane walls has not been attempted, as evidenced by a literature review. Adomian's decomposition method is used to solve a specific problem in section 2, and the results are presented in section 3. Section 4 examines the effect of various physical factors on velocity, temperature, and the rate of heat transfer on the walls of shrinking and stretching convergent/divergent channels. Section 4 is divided into two parts. A few concluding remarks about the provided work appear in Section 5.

2. Description of the problem

Between two non-parallel plane walls, an electrically conducting fluid is being considered for flow. It is necessary to apply magnetic field B_0 perpendicular to the radial axis of the walls. 2α is the angle at which these walls are positioned. At the point where two walls meet, there is either a source or a sink that causes the water to flow. Two-dimensional and one-directional flow is the norm. Flow is assumed to be symmetric around the central line, with $\theta = 0$, as well. Consequently, velocity is reduced to only the u component and is a function of both r and θ (theta being the polar angle). As a result, the components of velocity are $\mathbf{V} = (u, 0, 0)$.

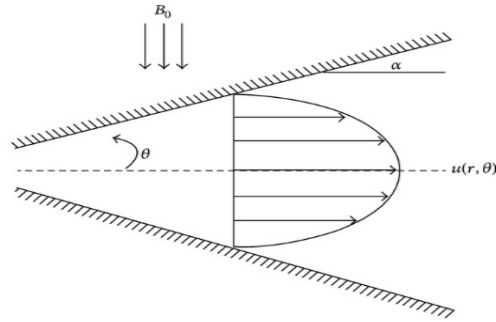


Figure 1: Geometry of the problem

In polar co-ordinates, the equations of motion and temperature in the presence of magnetic field and thermal radiation effects are.

$$\frac{\partial(ru)}{\partial r}, \quad (1)$$

$$u \frac{\partial u}{\partial r} = -\frac{1}{\rho} \frac{\partial p}{\partial r} + \nu \left[\frac{\partial^2 u}{\partial r^2} + \frac{1}{r} \frac{\partial u}{\partial r} + \frac{1}{r^2} \frac{\partial^2 u}{\partial \theta^2} - \frac{u}{r^2} \right] - \frac{\sigma B_0^2 u}{\rho r^2}, \quad (2)$$

$$-\frac{1}{\rho r} \frac{\partial p}{\partial \theta} + \frac{2\nu}{r^2} \frac{\partial u}{\partial \theta} = 0, \quad (3)$$

$$u \frac{\partial T}{\partial r} = \frac{\kappa}{\rho c_p} \left(\frac{\partial^2 T}{\partial r^2} + \frac{1}{r} \frac{\partial T}{\partial r} + \frac{1}{r^2} \frac{\partial^2 T}{\partial \theta^2} \right) + \frac{\nu}{c_p} \left(4 \left(\frac{\partial u}{\partial r} \right)^2 + \frac{1}{r^2} \left(\frac{\partial u}{\partial \theta} \right)^2 \right) + \frac{16}{3\rho K^* c_p r^2} T_w^3 \left(\frac{\partial^2 T}{\partial \theta^2} - \frac{\partial T}{\partial \theta} \right), \quad (4)$$

The suitable boundary conditions for the under-consideration problem at the middle line ($\theta = 0$) and at the walls ($\theta = \alpha$) are.

$$\frac{\partial u}{\partial \theta} = 0, \quad \frac{\partial T}{\partial \theta} = 0, \quad u = \frac{u_c}{r}, \quad (5)$$

$$u = u_w = \frac{s}{r}, \quad T = \frac{T_w}{r^2}, \quad (6)$$

Equations 2 to 6 include physical quantities such as the fluid temperature, kinetic viscosity and center-line velocity, as well as temperature at the walls, kinematic viscosity, stretching and shrinking, and specific heat under constant pressure. The letters $T, \kappa, p, T_w, \nu, s, u_c$ and c_p , are used to signify these values, respectively.

The dimensionless variables are defined as.

$$F(\eta) = \frac{f(\theta)}{u_c}, \quad \beta(\eta) = \frac{Tr^2}{T_w}, \quad \eta = \frac{\theta}{\alpha}. \quad (7)$$

The following system of nonlinear ordinary differential equations for velocity and temperature with transformed boundary conditions can be obtained by removing the pressure terms from Equations (2) and (3) and then using the nondimensional variable described by Equation (1).

$$F''' + 2\alpha Re F F' + (4 - Ha)\alpha^2 F' = 0, \quad (8)$$

$$(1 + Rd)\beta'' + 2\alpha^2(2 + PrF)\beta + \frac{PrEc}{Re}(4\alpha^2F^2 + F'^2) - \alpha Rd\beta' = 0, \quad (9)$$

$$F(0) = 1, F'(0) = 0, F(1) = C, \quad (10)$$

$$\beta'(0) = 0, \beta(1) = 1, \quad (11)$$

The nondimensional physical parameters embedded in Eqs. (8) and (9) are $Pr = \frac{\rho c_p u_c}{k}$, $Ec = \frac{\alpha u_c^2}{c_p T_w}$, $Re = \frac{\alpha u_c}{\nu}$, $Ha = \frac{\sigma B_0^2}{\rho \nu}$, and $Rd = \frac{16\sigma^* T_\infty^3}{3kk^*}$ and these are Prandtl, Eckert, Reynold's, Hartmann and Radiation numbers, respectively. Also, C is the stretching/shrinking parameter and $C > 0$ correspond to stretching and $C < 0$ for shrinking of the channel walls. Another important parameter known as convergent/divergent parameter is α . For divergent channel $\alpha > 0$, while, for convergent channel $\alpha < 0$.

The expression for the rate of heat transfer (local Nusselt number) at the walls of the channel is.

$$\alpha r^2 Nu = -\beta'(1).$$

3. Solution of the problem

So, we focused on analytical solutions to the under-consideration problem because the exact solutions for nonlinear differential equations are so amazing to think about. A technique called as Adomian's decomposition approach is used for this purpose. Eqs. (8) and (9) can be written in the typical approach of Adomian's decomposition method as follows:

$$L_1 F = -(2\alpha Re FF' + (4 - Ha)\alpha^2 F'), \quad (12)$$

$$L_2 F = -\frac{1}{1+Rd} (2\alpha^2(2 + PrF)\beta + \frac{PrEc}{Re}(4\alpha^2 F^2 + F'^2) - \alpha Rd\beta'), \quad (13)$$

where L_1 and L_2 are linear differential operators and for Eqs. (8) and (9) these operators are $L_1 = \frac{d^3}{d\eta^3}$ and $L_2 = \frac{d^2}{d\eta^2}$, respectively. The inverse operators of L_1 and L_2 are $L_1^{-1} = \int_0^\eta \int_0^\eta \int_0^\eta (\cdot) d\eta d\eta d\eta$ and $L_2^{-1} = \int_0^\eta \int_0^\eta (\cdot) d\eta d\eta$. Applying these inverse operators on Eqs. (12), (13) and consuming the boundary conditions we arrive with the following form;

$$F = 1 + \frac{\eta^2}{2!} M - \int_0^\eta \int_0^\eta \int_0^\eta (2\alpha Re FF' + (4 - Ha)\alpha^2 F') d\eta d\eta d\eta, \quad (14)$$

$$\beta = N - \frac{1}{1+Rd} \int_0^\eta \int_0^\eta \left(2\alpha^2(2 + PrF)\beta + \frac{PrEc}{Re}(4\alpha^2 F^2 + F'^2) - \alpha Rd\beta' \right) d\eta d\eta, \quad (15)$$

where M and N are constants that can be calculated by remaining boundary conditions. By choosing $F_0 = 1 + \frac{M\eta^2}{2!}$ and $\beta_0 = N$, as an infant approximation for F and β and then the recursive relation for higher order approximations of the solutions are in the following manner;

$$F_{k+1} = - \int_0^\eta \int_0^\eta \int_0^\eta (2\alpha Re A_k + (4 - Ha)\alpha^2 F'_k) d\eta d\eta d\eta, \quad (16)$$

$$\beta_{k+1} = -\frac{1}{1+Rd} \int_0^\eta \int_0^\eta \left(4\alpha^2 \beta_k + 2\alpha^2 Pr B_k + \frac{PrEc}{Re} (4\alpha^2 C_k + D_k) - \alpha Rd \beta_k' \right) d\eta d\eta, \tag{17}$$

where A_k, B_k, C_k and D_k ($k = 0, 1, 2, 3, 4 \dots$) are Adomian's polynomials for nonlinear terms ingrained in the flow model. These Adomian's polynomials can be find out with the help of formula given below.

$$B_k = \frac{1}{k!} \frac{d^k}{d\lambda^k} \left\{ F \left(\sum_{r=0}^k \lambda^r u_r \right) \right\}_{\lambda=0}, \quad k \geq 0, \tag{18}$$

Analytical and numerical solutions for convergent and divergent channels are compared in Tables 1 and 2. As shown in the following Tables, Adomian's decomposition method and numerical solutions have better agreement with each other than previously thought.

Table 1: Comparison between ADM and Numerical solutions for convergent channel

η	$F(\eta)$		$\beta(\eta)$	
	<i>ADM</i>	<i>Numerical</i>	<i>ADM</i>	<i>Numerical</i>
0.0	1.0000000	1.0000000	1.0157366	1.0157366
0.1	0.9934230	0.9934230	1.0155976	1.0155976
0.2	0.9736348	0.9736348	1.0151787	1.0151787
0.3	0.9404642	0.9404642	1.0144744	1.0144744
0.4	0.8936327	0.8936327	1.0134742	1.0134742
0.5	0.8327629	0.8327629	1.0121632	1.0121632
0.6	0.7573933	0.7573933	1.0105209	1.0105209
0.7	0.6669974	0.6669974	1.0085206	1.0085206
0.8	0.5610091	0.5610091	1.0061291	1.0061291
0.9	0.4388560	0.4388560	1.0033053	1.0033053
1.0	0.3000000	0.3000000	1.0000000	1.0000000

Table 2: Comparison between ADM and Numerical solutions for divergent channel

η	$F(\eta)$		$\beta(\eta)$	
	<i>ADM</i>	<i>Numerical</i>	<i>ADM</i>	<i>Numerical</i>
↓				

0.0	1.0000000	1.0000000	1.0160237	1.0160237
0.1	0.9925577	0.9925577	1.0158844	1.0158844
0.2	0.9702948	0.9702948	1.0154633	1.0154633
0.3	0.9333994	0.9333994	1.0147520	1.0147520
0.4	0.8821738	0.8821738	1.0137370	1.0137370
0.5	0.8170180	0.8170180	1.0123999	1.0123999
0.6	0.7384080	0.7384080	1.0107187	1.0107187
0.7	0.6468686	0.6468686	1.0086677	1.0086677
0.8	0.5429435	0.5429435	1.0062185	1.0062185
0.9	0.4271612	0.4271612	1.0033402	1.0033402
1.0	0.2999999	0.2999999	1.0000000	1.0000000

4. Results and discussion

Here, using graphical aid, we investigate the effects of various nondimensional physical parameters such as Reynold's Re , Hartmann Ha , Prandtl, Pr , Eckert number Ec , Radiation number Rd , converging/diverging parameter α and stretching/shrinking parameter C on the non-dimensional velocity field $F(\eta)$, temperature field $\beta(\eta)$, and local Nusselt number (rate of heat transfer at the walls.)

As depicted in Figures 2-9, the velocity field $F(\eta)$, behaves differently in shrinking and stretching channels. It can be seen from Figure 1 and Figure 2 that for shrinking and stretching channels, the velocity profile is flat at the central region of the channel, whereas for converging channels, $F(\eta)$, shows an increasing trend. The effects of altering alpha on a diverging channel are reversed when the channel shrinks or stretches. When a diverging channel is contracting, the decrease in velocity is slower than when a divergent channel is stretching. A diverging canal generates backflow in the area of its walls. Figures 4 and 5 show how the $F(\eta)$, changes when the Hartmann number changes. Ha has a similar effect on velocity profiles in both shrinking and stretching channels, as shown by this comparison. Changing Reynold's number has an effect on the velocity field $F(\eta)$, as shown in Figures 6 and 7. Variations in Reynold's number have the opposite effect on $F(\eta)$, for shrinking and stretching convergent/divergent channels, as can be shown from these results. Increasing the Reynold's number in a stretching channel causes a quick reduction in velocity. For shrinking and stretching divergent channels, however, Reynold's number exerts a nearly identical influence on $F(\eta)$.

Figures 8 and 9 show the effects of C on velocity field $F(\eta)$, for convergent and divergent channels, respectively. Shrinkage ($C < 0$) and stretching ($C > 0$) have the opposite effect on the velocity field, as can be shown from these results. Compared to divergent channels, the velocity profile of a shrinking convergent channel degrades rapidly. Positive values of C in Figure 9 show growing $F(\eta)$, behaviour.

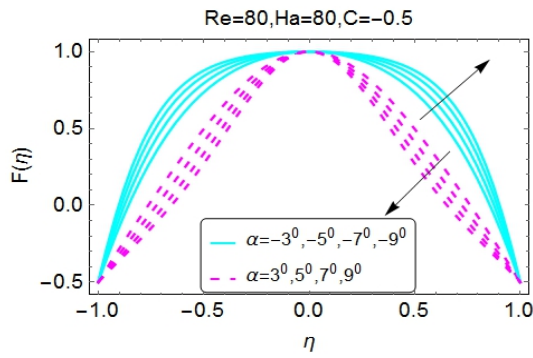


Figure 2: Influence of α on $F(\eta)$ in shrinking channel

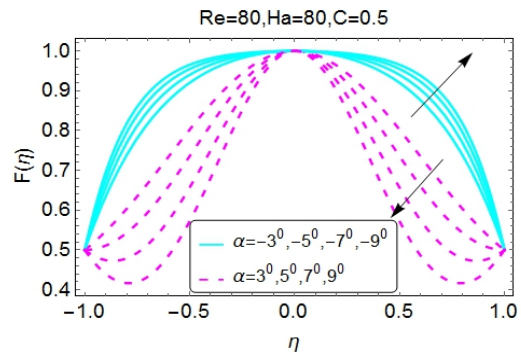


Figure 3: Influence of α on $F(\eta)$ in stretching channel

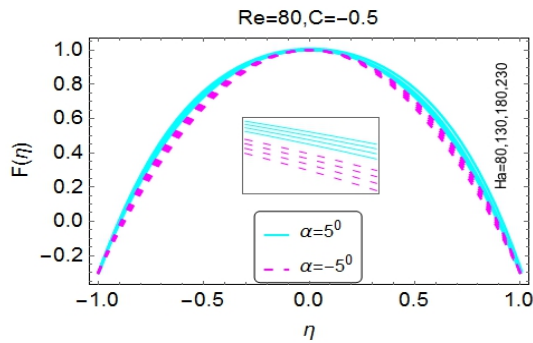


Figure 4: Influence of Ha on $F(\eta)$ in shrinking channel

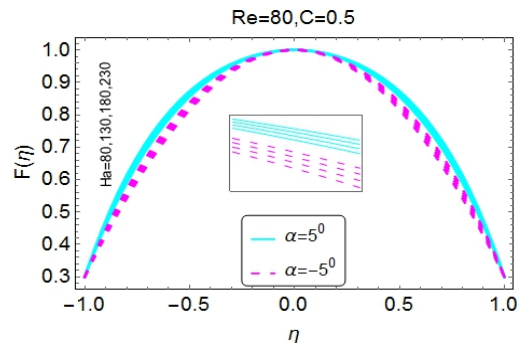


Figure 5: Influence of Ha on $F(\eta)$ in stretching channel

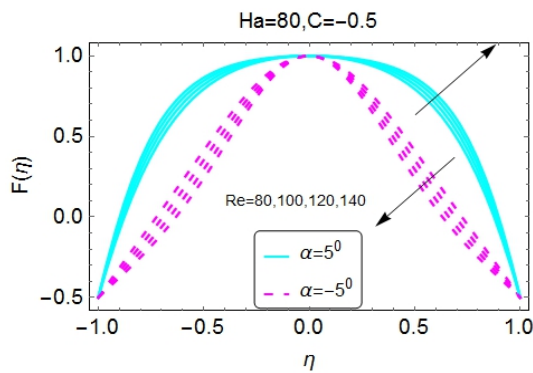


Figure 6: Influence of Re on $F(\eta)$ in shrinking channel

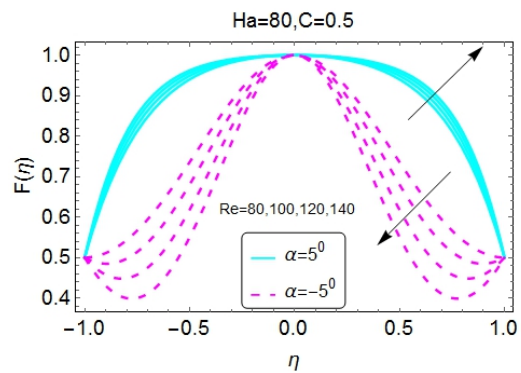


Figure 7: Influence of Re on $F(\eta)$ in stretching channel

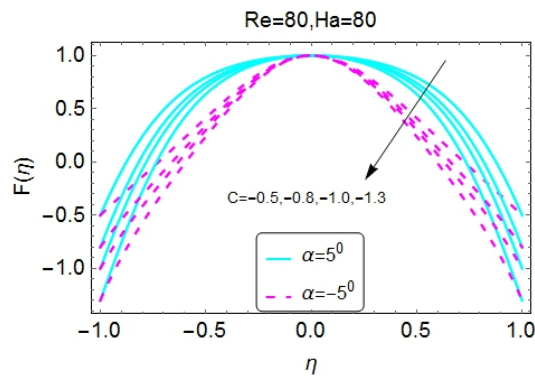


Figure 8: Influence of C on $F(\eta)$ in shrinking channel

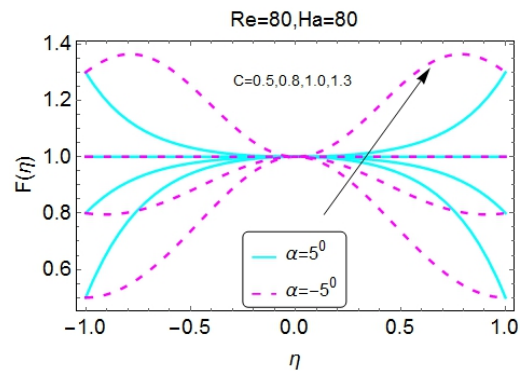


Figure 9: Influence of C on $F(\eta)$ in stretching channel

Figures 10-15 are shown to show how radiation number Rd , Prandtl number Pr Eckert number Ec affect the temperature field $\beta(\eta)$. Convergent/divergent channels can shrink and expand depending on the temperature of the surrounding environment.

Figures 10 and 11 show how the radiation number affects $\beta(\eta)$. When can be seen in these graphs, as the radiation number Rd increases, the temperature profile begins to decrease. Shrinkage and stretching convergent/divergent temperature profiles behave remarkably identically. Furthermore, the channel's temperature reaches its highest point in the center. There is a strong correlation between Prandtl number Pr and $\beta(\eta)$ as shown in Figures 12 and 13. These results show that the temperature field increases as the Prandtl number increases. When a channel shrinks, the temperature rises quickly; however, when a channel stretches, the temperature rise is much slower than in shrinking channels. The influence of Prandtl number on temperature diminishes as we travel away from the central line ($\eta = 0$) toward the channel walls ($\eta = 1$). A plot of varying Eckert numbers on a non-dimensional temperature $\beta(\eta)$ is shown in Figures 14 and 15. Temperature rises as Eckert number grows in both figures. In comparison to stretching channels, the rate of increase is much slower for shrinking channels. Furthermore, the core portion of the channel's temperature rises relatively slowly when lengthening channels.

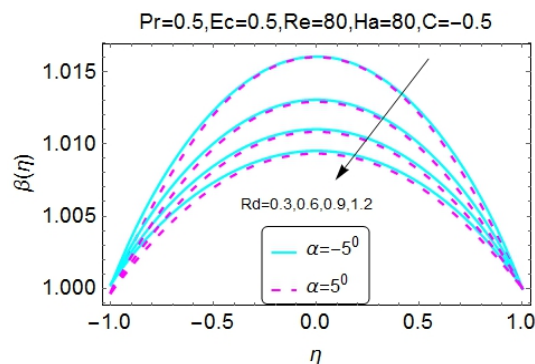


Figure 10: Influence of Rd on $\beta(\eta)$ in shrinking channel

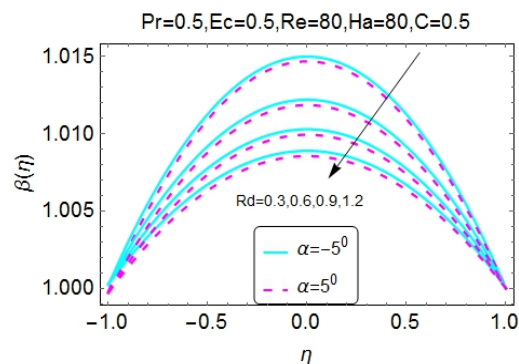


Figure 11: Influence of Rd on $\beta(\eta)$ in stretching channel

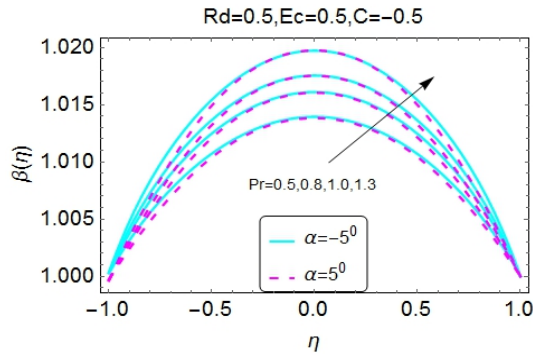


Figure 12: Influence of Pr on $\beta(\eta)$ in shrinking channel

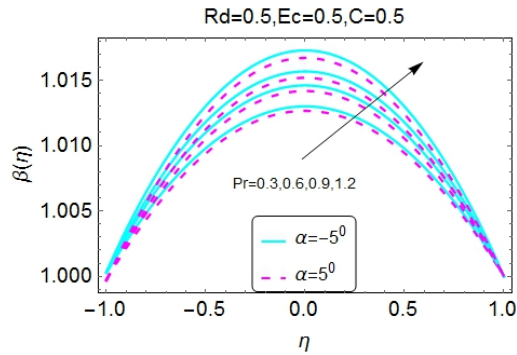


Figure 13: Influence of Pr on $\beta(\eta)$ in stretching channel

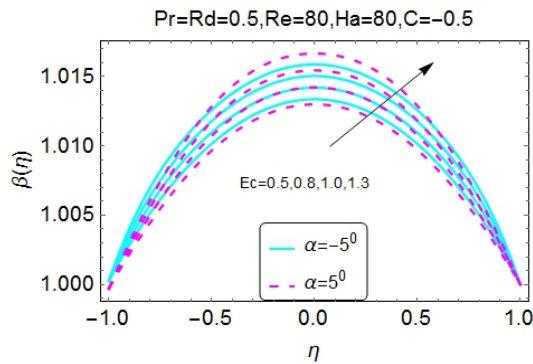


Figure 14: Influence of Ec on $\beta(\eta)$ in shrinking channel

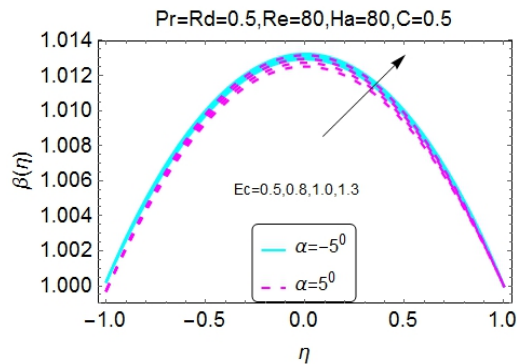


Figure 15: Influence of Ec on $\beta(\eta)$ in stretching channel

The rate of heat transmission at the channel walls is strongly influenced by nondimensional physical characteristics. Figures 16-21 are plotted for this purpose. An illustration of how radiation number, Prandtl number, and Eckert number affect heat transfer rates at walls can be seen in these diagrams. Discussing the examples of convergent and divergent channels.

Figures 16 and 17 show how the rate of heat transmission for convergent and divergent channels differs depending on the value of the radiation number. From these two diagrams, it can be shown that heat transfer rates decrease with increasing radiation number values. As contrast to the convergent channel, the rate of heat transmission in the divergent channel decreases faster. Figures 18 and 19 show the impact of altering the Eckert number on the Nusselt number. The growing behaviour in convergent and divergent channels may be seen in the Nusselt number, which is derived from this data. There is increased heat transmission at the channel walls for diverging channels. A heat transmission rate is shown in Figures 20 and 21 by comparing the Prandtl and Eckert figures. Figures 20 and 21 show that the rate of heat transfer is nearly identical for convergent and divergent channels.

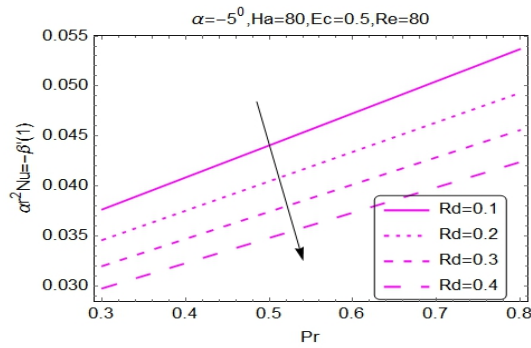


Figure 16: Influence of Rd on $-\beta'(1)$ in convergent channel

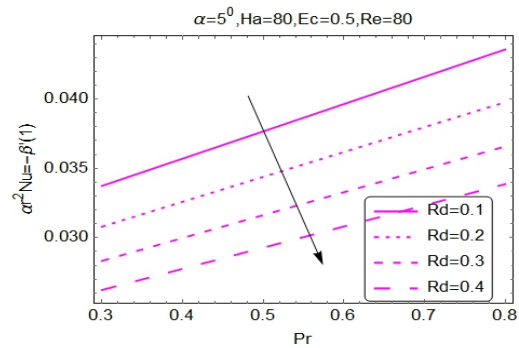


Figure 17: Influence of Rd on $-\beta'(1)$ in divergent channel

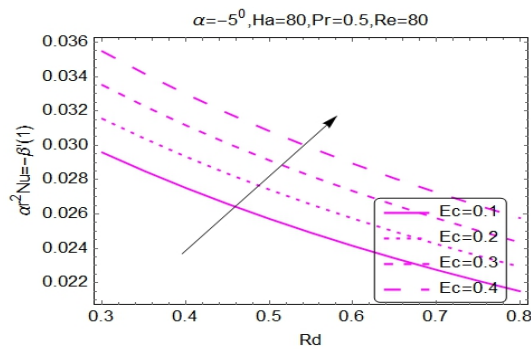


Figure 18: Influence of Ec on $-\beta'(1)$ in convergent channel

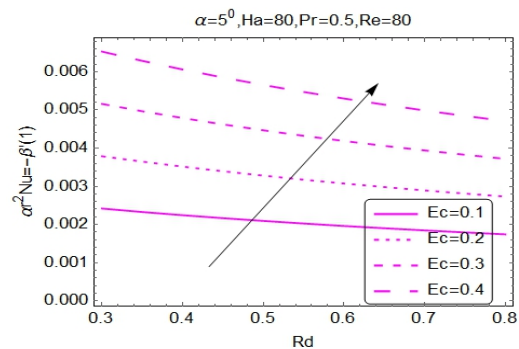


Figure 19: Influence of Ec on $-\beta'(1)$ in divergent channel

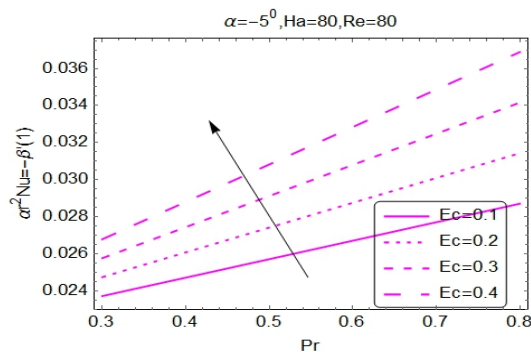


Figure 20: Influence of Ec and Pr on $-\beta'(1)$ in convergent channel

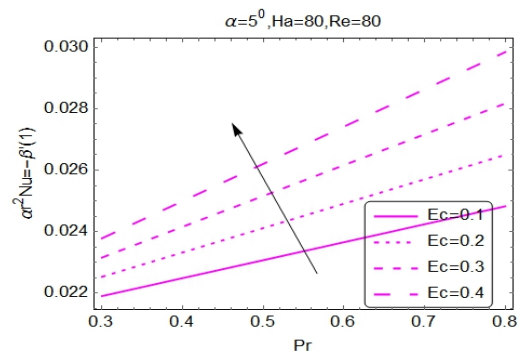


Figure 21: Influence of Ec and Pr on $-\beta'(1)$ in divergent channel

5. Conclusions

On the flow of viscous incompressible fluid between two nonparallel plane walls, the effects of magneto-hydrodynamics and heat radiation are explored in this article. Flow between convergent and divergent channels is another name for this sort of flow, as is Jeffery-Hamel flow. Adomian's decomposition approach is used to calculate the flow model's solutions. Nondimensional physical characteristics have an impact on velocity, temperature, and heat transfer rates, and the following conclusions are drawn from this investigation.

1. The velocity field remains flat in the center of the channel for both shrinking and stretching channels when a converging/diverging parameter α is varied, however backflow occurs at the channel walls when the walls are stretched.
2. In shrinking and stretching channels, differences in velocity profiles are observed for a wide range of Hartmann numbers.
3. Variations in Reynold's number are observed in the velocity field reversals, although in a stretched channel these variations are more rapid than in a decreasing channel.
4. When shrinking ($C > 0$) or stretching ($C < 0$), the velocity profile is affected in the opposite way by the C parameter.
5. The temperature field reverses when Radiation and Prandtl numbers are varied. The temperature field rapidly decreases as the radiation number is elevated.
6. When the Eckert number in the stretching channel is bigger, the temperature increases more slowly.
7. Convergent and divergent channels both experiences decreased heat transfer at the walls due to differences in radiation number.
8. In both convergent and divergent channels, an increase in the rate of heat transfer at the walls is observed for varying Eckert numbers.
9. In the case of convergent and divergent channels, analytical and numerical results are in perfect harmony.

References

- [1] G. B. Jeffery, "The two-dimensional steady motion of a viscous fluid," *Philosophical Magazine Series 6*, **29**(172), 455-465 (1915).
- [2] Hamel G, "Spiralformige Bewegungen zaher Flussigkeiten," *Jahresbericht der deutschen mathematiker-vereinigung*, **25**, 34–60 (1916).
- [3] S. T. Mohyud-Din, U. Khan, N. Ahmed and H. S. M, "Magnetohydrodynamic Flow and Heat Transfer of Nanofluids in Stretchable Convergent/Divergent Channels," *Applied Sciences*, **5**, 1639-1664 (2015).
- [4] S. T. Mohyud-Din, U. Khan, N. Ahmed and W. Sikander, "A Study of Velocity and Temperature Slip Effects on Flow of Water Based Nanofluids in Converging and Diverging Channels," *International Journal of Applied and Computational Mathematics*, **1**(4), 569–587 (2015).
- [5] H. Z. Poor, H. Moosavi, A. Moradi and M. Parastarfeizabadi, "On Thermal Radiation Effect in the MHD Jeffery-Hamel Flow of a Second Grade Fluid," *International Journal for Research in*

- applied science and engineering technology*, **2**(vii), 219-233 (2014).
- [6] T. Hayat, M. Nawaz, S. Asghar and A. A. Hendi, "Series solution for flow of a second grade fluid in a divergent-convergent channel," *Can J. Physics*, **88**, 911-917 (2010).
- [7] U. Khan, N. Ahmed and S. T. Mohy-ud-Din, "Soret and Dufour effects on flow in converging and diverging channels," *Aerospace Science and Technology*, **49**, 135-143 (2016).
- [8] S. A. El-Wakil and M. A. Abdou, "New applications of variational iteration method using Adomian polynomials," *Nonlinear Dynamics*, **52**(1), 41-49 (2008).
- [9] M. O. Olayiwola, "The Variational Iteration Method for Analytical Treatment of Homogeneous and Inhomogeneous Partial Differential Equations," *Global Journal of Science Frontier Research*, **15**(1), 2015.
- [10] T. A. Adeosun, O. J. Fenuga, S. O. Adelana, M. A. John, O. Olalekan and B. K. Alao, "Variational Iteration Method Solutions for Certain Thirteenth Order Ordinary Differential Equations," *Physics & Mathematics*, **4**(10), 1405-1411 (2013).
- [11] A. S. J. AL-Saif and T. A. K. Hattim, "Variational Iteration Method for Solving Some Models of," *International Journal of Pure and Applied Sciences and Technology*, **4**(1), 30-40 (2011).
- [12] S. T. Mohyud-Din, M. A. Noor and A. Waheed, "Variation of Parameters Method for Initial and Boundary Value Problems," *World Applied Sciences Journal*, **11**(5), 622-639 (2010).
- [13] S. T. Mohyud-Din, M. A. Noor and A. Waheed, "Variation of parameters method for solving sixth-order boundary value problems," *Communications of the Korean Mathematical Society*, **24**, 605-615 (2009).
- [14] Z. A. Zaidi, S. U. Jan, N. Ahmed, U. Khan and S. T. Mohyud-Din, "Variation of Parameters Method for Thin film Flow of a third Grade fluid down an Inclined Plane," *italian journal of pure and applied mathematics*, **31**(31), 161-168 (2013).
- [15] R. Grzymkowski, M. Pleszczyński and D. Słota, "Comparing the Adomian decomposition method and the Runge–Kutta method for solutions of the Stefan problem," *International Journal of Computer Mathematics*, **83**(4), 409-417 (2006).
- [16] A. M. Wazwaz, "The modified decomposition method for analytic treatment of differential equations," *Applied Mathematics and Computation*, **173**(1), 165–176, 2006.
- [17] D. Lesnic and L. Elliott, "The Decomposition Approach to Inverse Heat Conduction," *Journal of Mathematical Analysis and Applications*, **232**(1), 82-98 (1999).
- [18] X. G. Luo, Q.-B. Wu and B.-Q. Zhang, "Revisit on partial solutions in the Adomian decomposition method: Solving heat and wave equations," *Journal of Mathematical Analysis*

- and Applications*, **321**(1), 353-363 (2006).
- [19] M. Esmailpour and D. G. D, "Solution of the Jeffery–Hamel flow problem by optimal homotopy asymptotic method," *Computers & Mathematics with Applications*, **59**(11), 3405-3411 (2010).
- [20] S. J. Liao, "Numerically solving non-linear problems by the homotopy analysis method," *Computational Mechanics*, **20**(6), 530-540 (1997).
- [21] S. Liao, "On the homotopy analysis method for nonlinear problems," *Applied Mathematics and Computation*, **147**, 499–513 (2004).
- [22] S. S. Motsa, P. Sibanda, F. G. Awad and S. Shateyi, "A new spectral-homotopy analysis method for the MHD Jeffery–Hamel problem," *Computers & Fluids*, **39**(7), 1219–1225 (2010).
- [23] A. A. Joneidi, D. D. Ganji and M. Babaelahi, "Differential Transformation Method to determine fin efficiency of convective straight fins with temperature dependent thermal conductivity," *International Communications in Heat and Mass Transfer*, **36**(7), 757–762 (2009).
- [24] R. Bellman, B. G. Kashef and J. Casti, "Differential quadrature: A technique for the rapid solution of nonlinear partial differential equations," *Journal of Computational Physics*, **10**(1), 40-52 (1972).
- [25] A. Arikoglu and I. Ozkol, "Solution of difference equations by using differential transform method," *Applied Mathematics and Computation*, **174**(2), 1216–1228 (2006).
- [26] S. M. Moghimi, D. D. Ganji, H. Bararnia, M. Hosseini and M. Jalaal, "Homotopy perturbation method for nonlinear MHD Jeffery–Hamel problem," *Computers & Mathematics with Applications*, **61**(8), 2213–2216 (2011).
- [27] M. A. Noor and S. T. Mohyud-Din, "Homotopy perturbation method for solving sixth-order boundary value problems," *Computers & Mathematics with Applications*, **55**, 2953–2972 (2008).